The Auk 127(3):590–604, 2010
© The American Ornithologists' Union, 2010.
Printed in USA.

HOMOLOGY AND EVOLUTION OF AVIAN COMPOUND RHAMPHOTHECAE

TOBIN L. HIERONYMUS[1,2,3] AND LAWRENCE M. WITMER[2]

[1]*Department of Biological Sciences, Ohio University, Athens, Ohio 45701, USA; and*
[2]*Department of Biomedical Sciences, Ohio University College of Osteopathic Medicine, Athens, Ohio 45701, USA*

ABSTRACT.—We show that the topology of separate elements in avian compound rhamphothecae are strongly similar among different clades, not only in external appearance but in how these elements conform to underlying structures. We conducted a morphological survey of 81 extant bird species and tested superficial similarities in external beak morphology for substantive similarity in associated skeletal structures and nerve courses. A revised set of morphological characters for compound rhamphothecae was optimized onto three recent phylogenetic trees to assess the relationships of homology and homoplasy in rhamphothecal morphology. Osteological correlates of rhamphothecae from the extinct basal ornithurine birds *Hesperornis* and *Ichthyornis* show that compound rhamphothecae are the primitive state for the clade including extant birds (Neornithes). Simple rhamphothecae are the result of the loss of softer keratinous grooves between rhamphothecal components, and there are many examples of transitional forms between compound and simple rhamphothecae in which the grooves remain as shallow depressions without a pronounced edge. Ancestral-character-state reconstructions of rhamphothecal morphology within Neornithes also show a considerable amount of homoplasy. We suggest that frequent homoplasy in rhamphothecal morphology is the result of underlying similarity in facial development. *Received 13 April 2009, accepted 13 November 2009.*

Key words: anatomy, ancestral state reconstruction, functional morphology, homology, homoplasy, rhamphotheca.

Homologie et évolution du revêtement corné complexe des oiseaux

RÉSUMÉ.—La topologie d'éléments distincts du revêtement corné complexe des oiseaux est fortement similaire entre différents clades, non seulement dans leur apparence externe mais aussi dans la façon dont ces éléments correspondent aux structures sous-jacentes. Nous avons réalisé une étude morphologique de 81 espèces d'oiseaux modernes et testé si les similarités de la morphologie externe du bec étaient reliées à une importante similarité des structures squelettiques associées et des nerfs. Une nouvelle série de caractères morphologiques du revêtement corné complexe a été optimisée sur trois arbres phylogénétiques récents afin d'évaluer les relations d'homologie et d'homoplasie de la morphologie du revêtement corné. Les corrélations ostéologiques du revêtement corné de *Hesperornis* et *Ichthyornis*, des oiseaux ornithurines éteints, montrent que les revêtements cornés complexes correspondent à l'état primitif du clade comprenant les oiseaux modernes (Néornithes). Les revêtements cornés simples sont le résultat de la perte de rainures de kératine plus molles entre les composantes du revêtement corné. Il existe de nombreuses formes de transition entre des revêtements cornés simples et complexes, pour lesquelles les rainures demeurent des dépressions peu profondes sans rebord prononcé. Des reconstructions des caractères morphologiques ancestraux du revêtement corné de Néornithes présentent aussi beaucoup d'homoplasie. Nous suggérons qu'une homoplasie fréquente de la morphologie du revêtement corné résulte d'une similarité sous-jacente du développement facial.

RHAMPHOTHECAE, THE HORNY (keratinous) sheaths that cover the jaws in birds, show amazing diversity and provide some of the most compelling and easily appreciated examples of morphological adaptation in vertebrates (Storer 1960), such as forceps for probing in sandpipers, filters in ducks and flamingos, "teeth" for gripping fish in mergansers and gannets, and nutcrackers in hawfinches. A widely distributed feature of rhamphothecae that appears to be unrelated to their adaptive roles in feeding and display can be seen in birds such as albatrosses, in which the skin of the rhamphotheca is separated into several plates (Fig. 1). This condition, referred to as a "compound rhamphotheca," contrasts with the continuous cornified sheaths seen in birds such as American Crows that possess a simple rhamphotheca (scientific names of all species in the study are given in the Appendix). Although some adaptive explanations have been suggested for compound rhamphothecae, the proposed explanations (such as providing a channel for excretions from the nasal salt gland in marine birds; Schmidt-Nielsen and Fänge 1958) are most often invoked for specific clades (e.g., procellariiform birds) and do not extend to all cases of compound rhamphothecae (e.g., to ratites).

---

[3] E-mail: thieronymus@neoucom.edu

The Auk, Vol. 127, Number 3, pages 590–604. ISSN 0004-8038, electronic ISSN 1938-4254. © 2010 by The American Ornithologists' Union. All rights reserved. Please direct all requests for permission to photocopy or reproduce article content through the University of California Press's Rights and Permissions website, http://www.ucpressjournals.com/reprintInfo.asp. DOI: 10.1525/auk.2010.09122

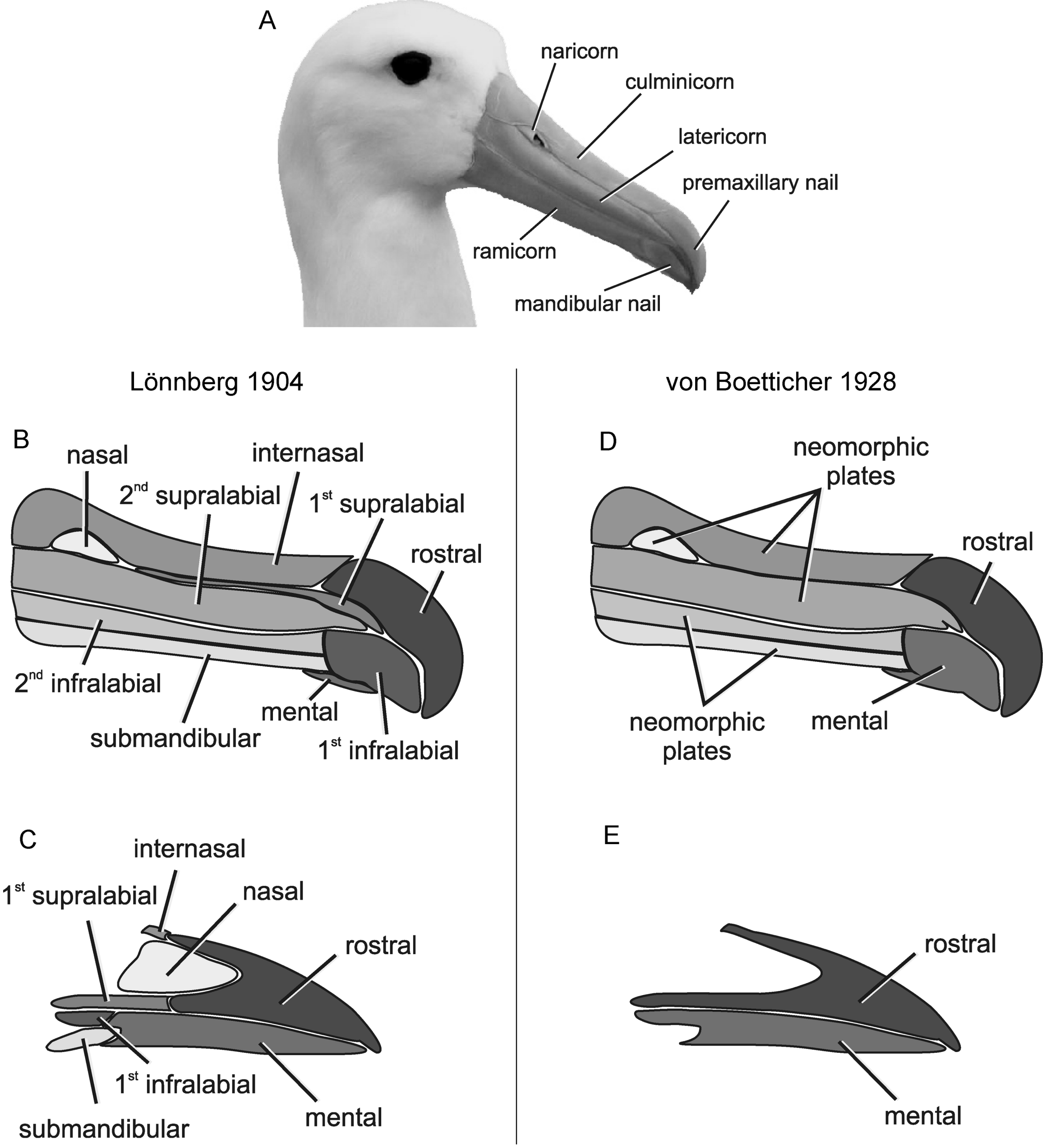

Fig. 1. (A) Nomenclature for separate plates of the compound rhamphotheca shown in a Waved Albatross (*Phoebastria irrorata*). Terms used here are largely derived from the nomenclature used by Coues (1866) to describe beak plates in Procellariiformes. Coues's "maxillary nail" has been changed to "premaxillary nail" to reflect the topological relationship between premaxilla and maxilla in the bony upper jaw. (B, C) Hypothesis of homology between areas of the rhamphotheca proposed by Lönnberg (1904), shown on the outlines of (B) Laysan Albatross and (C) American Crow. Lönnberg's (1904) hypothesis presents these elements as the result of fusion or reduction of the labial scales of squamates. (D, E) Von Boetticher's (1928) hypothesis of homology between rhamphothecal plates. This hypothesis used the sequence of development in rhamphothecal plates to resolve ambiguity in character polarization, selecting a simple rhamphotheca with only rostral and mental plates as primitive for Neornithes because these plates are the first to appear during development. Although von Boetticher (1928) recognized strong similarity between different examples of compound rhamphothecae, these similarities were cast as independent, convergent examples of additional beak plates. Source image of Waved Albatross licensed to James Lloyd under CC-BY-SA 3.0.

Birds traditionally considered to bear compound rhamphothecae (Gadow and Selenka 1891) are scattered throughout most published avian phylogenies. This distribution has led to conflicting views on the nature of compound rhamphothecae and whether the disparate examples are indeed homologous (Lönnberg 1904) or only superficially similar convergent structures (Parkes and Clark 1966). Understanding the evolutionary and morphological relationships between compound and simple rhamphothecae provides insight into the morphology and "evolvability" of bird beaks and may ultimately shed light on the early evolution of rhamphothecae from other skin structures in derived coelurosaurian dinosaurs.

Avian compound rhamphothecae have long been used as taxonomic characters. The most prominent system of nomenclature for elements of compound rhamphothecae was first proposed in the context of procellariiform seabird taxonomy (Coues 1866). Coues's (1866) nomenclature will be used here, with minor changes and additions (Fig. 1A).

The initial proposal of homology between separate plates in compound rhamphothecae was advanced as part of a hypothesis that rhamphothecal plates were homologous with the facial scales of other reptiles, most notably lizards and snakes (Lönnberg 1904). Although this work provided an extensive review of rhamphothecal morphology, it did not present the observed similarities in phylogenetic context. This omission is understandable, given that the evolutionary relationships of higher-order bird clades were poorly resolved at the time. In addition, Lönnberg's (1904) work employed only data from external rhamphothecal morphology. As such, this hypothesis of similarity between rhamphothecal plates (Fig. 1B, C) provides a useful starting point for testing morphological similarity, but not a rigorous test of homology.

A later monograph on avian beak morphology (von Boetticher 1928) describes a more thorough test of Lönnberg's (1904) hypothesis, with the inclusion of ontogenetic data and a more explicit phylogenetic context. Von Boetticher (1928) rejected many of the similarities discussed by Lönnberg (1904) and proposed a more limited hypothesis (Fig. 1D, E). Von Boetticher's (1928) test is still limited by current standards of homology testing, because of a poorly resolved phylogenetic hypothesis and an emphasis on similar development (as opposed to synapomorphy) as the arbiter of homology.

Here, we independently test Lönnberg's (1904) and von Boetticher's (1928) hypotheses of homology, supplemented with the inclusion of data that have bearing on the topology of structures associated with the rhamphotheca, namely branches of the trigeminal nerve and bony elements of the upper and lower jaws. We employ current phylogenetic hypotheses to reconstruct the ancestral character state of the avian beak at the common ancestor of extant birds (Neornithes) and frame these results within the context of currently accepted tests of homology and the biological basis of homology.

METHODS

Morphological survey.—We examined external rhamphothecal morphology in a broad sample of study skins and fixed alcoholic specimens (see Appendix for list of taxa). This broad survey was complemented by more extensive study on a smaller sample of taxa. Fourteen species were examined by micro-computed tomography (μCT) using a GE eXplore Locus Small Animal μCT Scanner. The resulting volume data (in VFF format) were exported from MICROVIEW, version 2.1.2 (microview.sourceforge.net), in DICOM format and imported into AMIRA, versions 3.1.1 and 4.1.1 (Mercury-TGS, Chelmsford, Massachusetts), for visualization. Of the 14 scanned specimens, 8 were prepared with radiopaque arterial or venous injections (Microfil MV series fill compounds, Flow Tech, Carver, Massachusetts) to examine patterns of vascularity in the rostrum. Five of the injected specimens were dissected to directly examine the soft tissues of the dermis beneath the rhamphotheca.

Samples from the five dissected specimens were fixed in neutral phosphate-buffered formalin, dehydrated in a series of ethanol baths, then infiltrated and embedded with polymethylmethacrylate (PMMA) resin using a protocol modified from Sterchi and Eurell (1989). Embedded samples were rough cut on a high-speed tile saw (D24000, DeWalt, Baltimore, Maryland), then serially sectioned using a variable-speed diamond wafering saw (Isomet 1000, Buehler, Lake Bluff, Illinois) at 800-μm intervals. The resulting sections were mounted on cast acrylic slides with cyanoacrylate glue, then ground and polished to a thickness of ~100 μm on a lapidary wheel (Metaserv 2000, Buehler) as semithin sections for histological analysis.

Study skins can sometimes offer a deceptive picture of the rhamphotheca and surrounding skin because softer skin tends to shrink more as it dries. Study skins may thus show grooves and folds in the rhamphotheca that are not present in living animals. Where possible, study skins were compared with alcoholic or frozen specimens.

It is difficult to distinguish the fusion of two rhamphothecal plates from the loss of one rhamphothecal plate in a phylogenetic comparative analysis using morphological data alone. In addition, the morphological differences in this anatomical system between taxa generally involve differences in the depth or extent of the grooves that separate rhamphothecal plates, not necessarily differences in the shapes of the plates themselves. Thus, it is more useful to consider and describe the structure of the grooves and folds on the rhamphotheca than the areas of homogeneous skin that make up a "rhamphothecal plate." We propose a nomenclature for the grooves in compound rhamphothecae and describe these structures in detail in the next section.

The survey of rhamphothecal morphology was complemented by a survey of osteological specimens to establish the bony morphology present beneath rhamphothecae in the study taxa (specimens listed in Appendix). In those cases in which osteological specimens of the species examined for soft-tissue morphology were not available, skeletons of congeneric specimens were examined as approximations.

Testing homology.—Our assessment of homology follows that of Patterson (1982), using the criteria of (1) strong similarity, (2) nonconjunction, and (3) congruence (or synapomorphy) to test the superficial similarities observed by Lönnberg (1904) and von Boetticher (1928). Strong similarity, as used here, incorporates a set of concepts used by previous workers as primary criteria for homology, including the criteria of relative position and continuity proposed by A. Remane (1955) and J. Remane (1983). The tests of similarity and conjunction directly employ data from the morphological survey. The test of congruence employs an assessment of synapomorphy based on the ancestral-character-state reconstructions of rhamphothecal morphology discussed in the following subsection.

The morphological similarities found in the present study will also be discussed in the context of the biological basis of similarity and homology, after Sæther (1979), Roth (1991), Butler and Saidel (2000), and Hall (2003), as a means of describing strong similarity that fails the conjunction or congruence tests. In addition to the classical relationship of homology, there are several examples of "duplicated" features (e.g., the α and β subunits of hemoglobin) in which two features found in conjunction can be traced to a single evolutionary origin. Roth (1991) coined the term "iterative homology" to describe this pattern, which may provide a biological basis for the evolutionary origins of rhamphothecae.

Strong similarity in the absence of phylogenetic congruence may sometimes be demonstrated to arise from homologous developmental mechanisms, in a pattern described as "underlying synapomorphy" by Sæther (1979), "syngeny" by Butler and Saidel (2000), and "underlying homology" by Hall (2003). Underlying synapomorphy is also potentially present in compound rhamphothecae, as described in the next section.

Ancestral-character-state reconstruction.—Ancestral-character-state reconstruction provides a means to test for synapomorphy and congruence. Adult morphological features for separate regions of the rostrum were coded as multistate characters, using the following character states: (0) single rhamphothecal plate, (1) rhamphothecal plate continuous into adjacent region, (2) cere or apteria, and (3) feathered skin (pteryla). This four-state coding scheme was also recoded as a binary character set, with state 0 remaining unaltered and states 1–3 combined into a single character state. This recombination separates compound rhamphothecae (as state 0) from simple rhamphothecae or other skin (as state 1). Binary recoding is less descriptive but offers the advantage of reducing the amount of parameter estimation required by some comparative methods.

In addition to the sample of extant taxa, data from fossils representing two close outgroup taxa to living birds (*Ichthyornis* and two hesperornithiforms, *Hesperornis* and *Parahesperornis*) were included to polarize rhamphothecal characters within Neornithes (Martin 1984, 1987; Elzanowski 1991; Clarke 2004). The correlates between bony morphology and rhamphothecal morphology found in the present study were sufficiently robust to allow us to estimate the morphology of the rhamphotheca and other areas of cephalic skin for these fossil birds.

The phylogenetic hypotheses of Ericson et al. (2006), Livezey and Zusi (2006, 2007), and Hackett et al. (2008) were used for the higher-order topology of Neornithes. Relationships between taxa within terminal clades for these three hypotheses were resolved according to several smaller-scale phylogenetic hypotheses: Cracidae after Pereira et al. (2002) and Pereira and Baker (2004), Anseriformes after Livezey (1996, 1997) and Donne-Goussé et al. (2002), Procellariiformes after Kennedy and Page (2002), Alcidae after Thomas et al. (2004), and Bucerotidae after Kemp (1988). Forty-six of the taxa surveyed were included in this part of the analysis. Ancestral character states were reconstructed using both a maximum-parsimony (MP) algorithm (Maddison et al. 1984) and a maximum-likelihood (ML) algorithm (Schluter et al. 1997) in MESQUITE, version 2.71 (Maddison and Maddison 2009). Maximum-parsimony ancestral-character-state reconstruction used the original multistate character set. Maximum-likelihood ancestral-character-state reconstruction used the binary recoded character set to reduce the amount of parameter estimation required in analysis and to prevent overfitting. Symmetrical (Mk1) estimated rates of character state change were used for all characters in the ML analysis except for the infralabial groove, which showed significantly greater likelihoods using an asymmetrical two-parameter estimate for rate of character-state change.

Branch lengths for the tree topologies used in ML ancestral-character-state reconstruction were estimated by setting internodes to an age greater than or equal to the age of the oldest known ingroup fossil in millions of years (Benton and Donoghue 2007). Successively older internodes without confidently assigned ingroup fossil taxa for calibration were placed at least 5 ma below calibrated internodes. The inclusion of a 5-ma branch alleviates the problem of "forcing" the uncalibrated nodes into the ancestral state of their closest calibrated daughter node. The problem of forcing is especially relevant with the inclusion of the fossil taxa *Ichthyornis* and *Hesperornis* as outgroups to polarize character states within Neornithes. In addition to the calibrated trees, ML reconstructions were also run on the same topologies with all branch lengths set to 1 to model punctuational change, again with branch lengths estimated using the method of Pagel (1992), and finally using modified topologies that placed *Hesperornis* and *Ichthyornis* as sister taxa.

Results

Rhamphothecae show similar topologies among groups.—The superficial similarities in rhamphothecal morphology within Neornithes that Lönnberg (1904) and von Boetticher (1928) first pointed out are largely borne out by comparative osteological and neurological data. Most of the named components of compound rhamphothecae illustrated in Figure 1A show consistent relationships to specific structures in the rostrum, and these similarities will be described in detail in this section. Most individual rhamphothecal components thus pass the similarity test of homology proposed by Patterson (1982).

Nearly all examples of avian compound rhamphothecae show a complete groove that extends from the naris (nostril) to the oral margin, here termed the "nasolabial groove" (Fig. 2C, D). In taxa with well-defined rhamphothecal plates, such as procellariiform birds, the nasolabial groove separates the latericorn from the culminicorn and the premaxillary nail. Exceptions include some of the anatid waterfowl (e.g., Northern Shoveler), which show a premaxillary nail but lack a well-defined nasolabial groove to separate the remaining upper bill into latericorn and culminicorn (Fig. 2A). A persistent partial nasolabial groove can sometimes be seen in taxa that are classically considered to bear simple rhamphotheca (e.g., Striated Heron; Fig. 2E). The nasolabial groove may also extend caudally from the naris to the caudal margin of the rhamphotheca (e.g., Laysan Albatross; Fig. 2C). *Apteryx* presents an extreme example of this tendency, in that nearly all of the nasolabial groove lies caudal to the nostril.

The position of the nasolabial groove at the oral margin is closely approximated by the rostralmost extent of the premaxillomaxillary

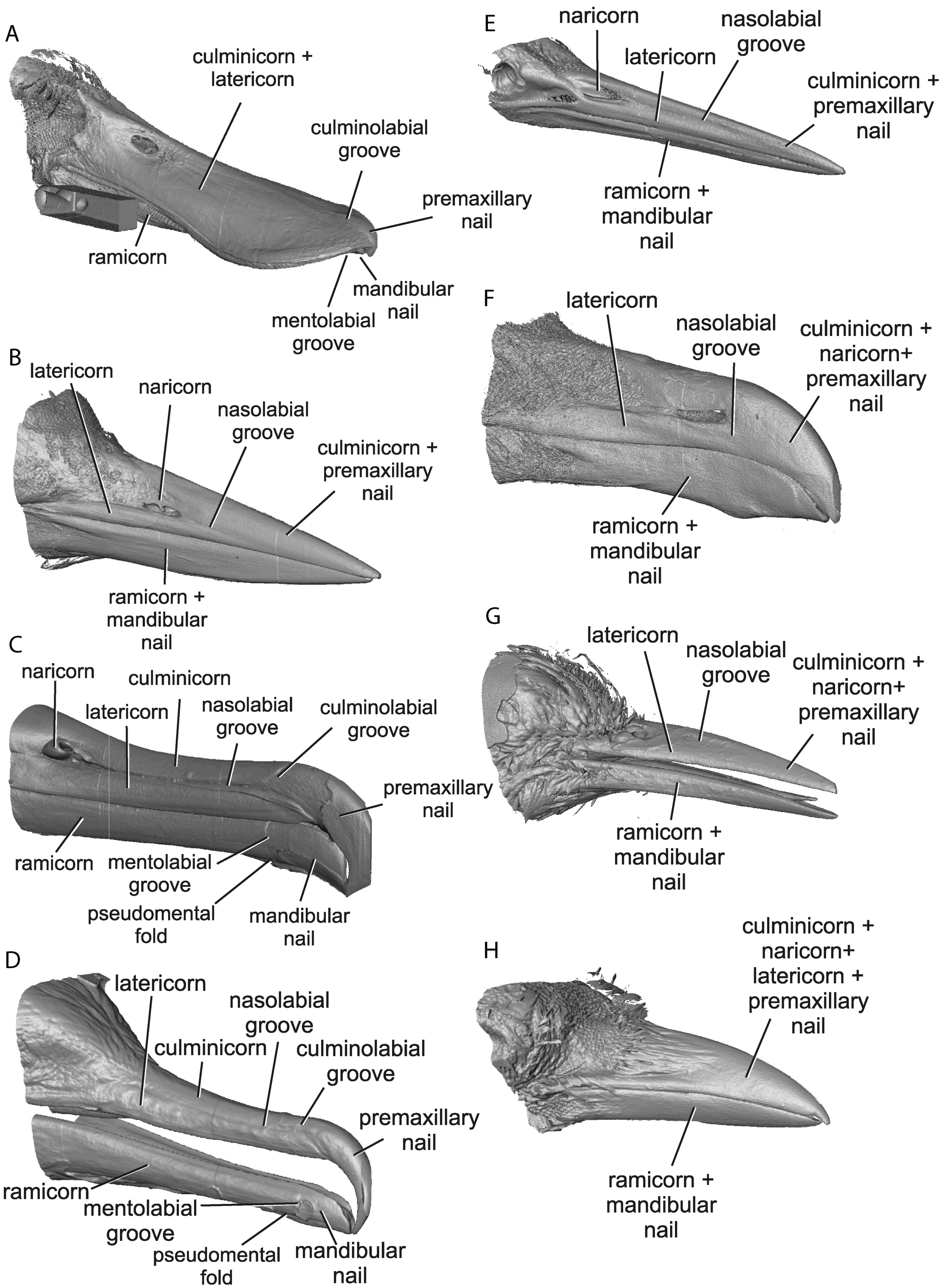

FIG. 2. Topographic anatomy of the rhamphotheca, showing rhamphothecal plates as well as nasolabial, culminolabial, and mentolabial grooves, in (A) Northern Shoveler, (B) Common Loon (*Gavia immer*), (C) Laysan Albatross, (D) Double-crested Cormorant, (E) Striated Heron, (F) Ring-billed Gull (*Larus delawarensis*), (G) Northern Flicker, and (H) American Crow (*Corvus brachyrhynchos*). Where the loss of a rhamphothecal groove results in fusion of plates, those plates are identified as composites (e.g., culminicorn + latericorn in Northern Shoveler). All images are surface renderings of CT scan data.

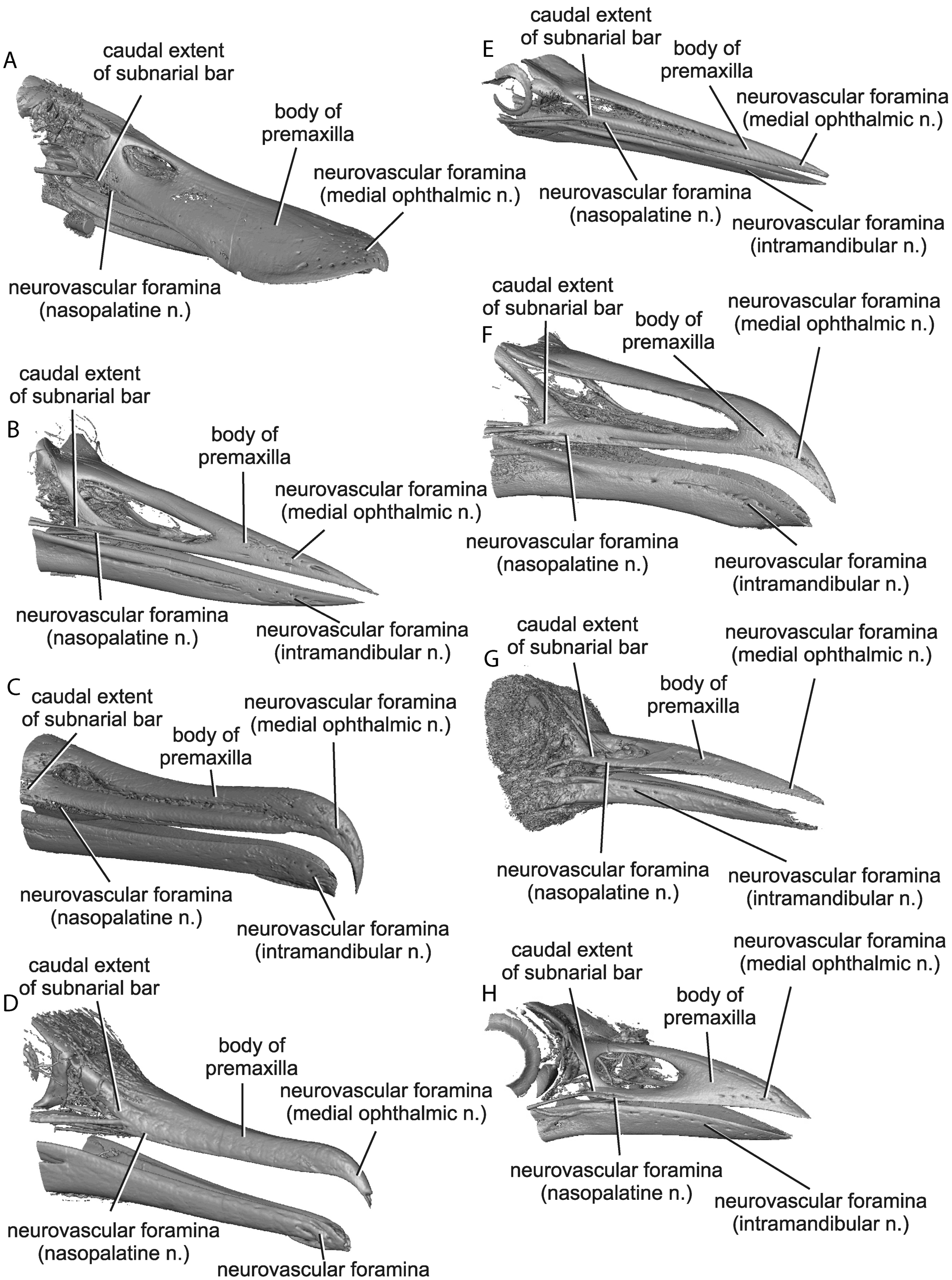

FIG. 3. Anatomy of the bony rostrum for individuals portrayed in Figure 2. Note that the subnarial bar of the premaxilla closely corresponds to the caudal extent of the latericorn in most taxa. Steganopode pelecaniforms, represented here by Double-crested Cormorant (D), are the only exception to this general rule. The neurovascular bundles that emerge from the caudalmost neurovascular foramina for the medial ophthalmic nerve generally continue under the rostral portion of the latericorn; in palaeognaths and galloanserine birds, the latericorn overlaps several of these neurovascular foramina (e.g., Northern Shoveler, A). All images are surface renderings of CT scan data.

suture. Taxa with pronounced nasolabial grooves (e.g., *Phoebastria*) often show a bony groove that corresponds to this skin feature (Fig. 3C). Bony correlates for the nasolabial groove are clearly visible in the fossil hesperornithiform bird *Hesperornis* (Elzanowski 1991).

The maxillary process (subnarial bar) of the premaxilla extends caudally beneath the nasolabial groove, usually as far as the caudal extent of the rhamphotheca (Fig. 3). Sutures between the subnarial bar and the maxilla are often obscured by bony fusion, but in all birds other than Galliformes, the ventral border of the subnarial bar invariably defines a series of foramina for the lateral branches of the nasopalatine nerve (Fig. 3). Galliform beaks are unusual in that the subnarial bar makes up the entire bony support for the edge or tomia of the maxillary rhamphotheca, obscuring the maxilla. Despite the occlusion of the rostral portion of the maxilla from the external surface of the upper jaw, the rostralmost extent of the maxilla corresponds to the position of the nasolabial groove fairly well. Some parts of the dorsal ramus of the medial ophthalmic nerve cross caudally beneath the nasolabial groove to innervate the rostral part of the latericorn (Fig. 3); thus, the nasolabial groove does not directly correspond to a border between the dermatomes of the medial ophthalmic (CN V_1) and nasopalatine (CN V_2) nerves.

Many taxa, both those with compound rhamphothecae such as procellariiform seabirds and those that have classically been considered to have simple rhamphothecae such as falconiform birds, show a groove that separates the premaxillary nail from the culminicorn, here termed the "culminolabial groove" (Fig. 2A, C, D). The culminolabial groove is often incomplete, in some cases fading out as it approaches the oral margin (e.g., *Fratercula*) and in others forming a shallow, indistinct depression (e.g., *Sula*). The most distinct examples of culminolabial grooves are found in anatoid waterfowl (e.g., Northern Shoveler; Fig. 2A), where the premaxillary nail is pronounced and heavily keratinized compared with the surrounding rhamphotheca.

In nearly all taxa with a compound mandibular rhamphotheca, a complete groove separates the mandibular nail from the ramicorn, here termed the "mentolabial groove." The position of this groove is variable but most often approximately matches the position of the nasolabial groove on the oral margin. In palaeognaths, the mentolabial groove is oriented rostrodorsal to caudoventral. In neognaths, the most common orientation of the mentolabial groove is dorsolateral to ventromedial. In both cases, the ventralmost portion of the mentolabial groove sits near the ventral border of the mandibular symphysis. Ibises (e.g., White-faced Ibis [*Plegadis chihi*]) are an exception to this pattern, showing a median groove and no well-defined mandibular nail.

An incomplete groove is present on the mandibular nail of Procellariiformes and members of Fregatidae, Phalacrocoracidae, Anhingidae, and Sulidae. The last four taxa form an unnamed monophyletic group in the analyses of Ericson et al. (2006) and Hackett et al. (2008); Livezey and Zusi (2007) place these taxa together with Pelecanidae in Steganopodes (Chandler 1916). For convenience, the four taxa that possess an incomplete groove on the mandibular nail will hereafter be referred to as "steganopode pelecaniforms" because they share this and a number of other rhamphothecal features in common to the exclusion of pelecanids. Where present, the incomplete groove continues along the line of the median caudal projection of the mandibular nail that von Boetticher (1928) termed the "pseudomentale"; thus, this incomplete groove is here termed the "pseudomental fold."

In *Casuarius*, Anatoidea, and some Procellariiformes, a second complete groove on the mandible mirrors the course of the nasolabial groove, extending from the mandibular malar pteryla to the mentolabial groove, here termed the "infralabial groove." This groove separates the ramicorn into dorsal and ventral parts. In many taxa, the infralabial groove is absent but a rostral projection of the mandibular malar pteryla makes a notch in the single ramicorn at a similar position. The position of the infralabial groove in *Casuarius* follows the course of the external mandibular vein, but the independently derived infralabial grooves in procellariiform seabirds and anatoid waterfowl accompany foramina for the intramandibular nerve.

Steganopode pelecaniforms show a novel groove that corresponds to the line of action of the prokinetic hinge in the jugal bar, delineating a separate beak plate termed the "jugal operculum" (MacDonald 1960). In all of the taxa examined, jugal opercula were accompanied by an accessory ossification, the suprajugal ossiculum (Jollie 1957), that attaches by a short ligament to the jugal as the latter overlaps the jugal process of the maxilla. Many of the osteological specimens examined in the present study retained the ligament, holding the suprajugal ossiculum in place in the prepared specimen. Although the suprajugal ossiculum is in proximity to the caudal extent of the subnarial bar of the premaxilla, there does not appear to be a ligament connecting the two structures; thus, the suprajugal ossiculum does not appear to be a separate center of ossification within the maxillary process of the premaxilla. This finding suggests that the close topological relationship between the caudal extent of the maxillary process of the premaxilla and the caudal end of the rhamphotheca seen in most avian taxa does not occur in steganopode pelecaniforms. It is unclear whether the jugal operculum formed as a sequential addition of a novel, discrete plate of cornified skin caudal to the

Fig. 4. (facing page) Maximum-parsimony (MP) and maximum-likelihood (ML) ancestral-character-state reconstructions for (A) distinct nasolabial grooves, (B) distinct culminolabial grooves, and (C) mentolabial grooves, shown for the higher-order topology of Hackett et al. (2008). Blue branches show the presence of grooves by significant ML reconstruction; blue asterisks at basal nodes show the presence of grooves by MP reconstruction. The rates of character-state change fitted by the ML reconstruction lead to uncertainty at the root of the tree (Ornithurae) for the state of nasolabial and culminolabial grooves, in contrast to the positive assessment of congruence by MP (asterisks). Although the character state for both sets of grooves on the upper jaw is uncertain for Neognathae and Neoaves by both ML and MP, the likelihood ratios for these nodes favor the presence of grooves as a primitive state (Table 1). By contrast, both MP and ML reconstructions of the mentolabial groove show congruence to the base of Neognathae and into Galloanserae. Some of the taxa on this tree retain a pronounced furrow between the nostril and the oral margin, which we interpret as a remnant of the nasolabial groove (e.g., *Colaptes auratus*, *Butorides striata*), and in some cases a similar furrow is accompanied by a second, indistinct furrow that we interpret as the remnant of the culminolabial groove (e.g., *Catharacta skua*, *Caloenas nicobarica*). Background colors follow the international standard for chronostratigraphic units proposed by the Commission for the Geological Map of the World (see Acknowledgments).

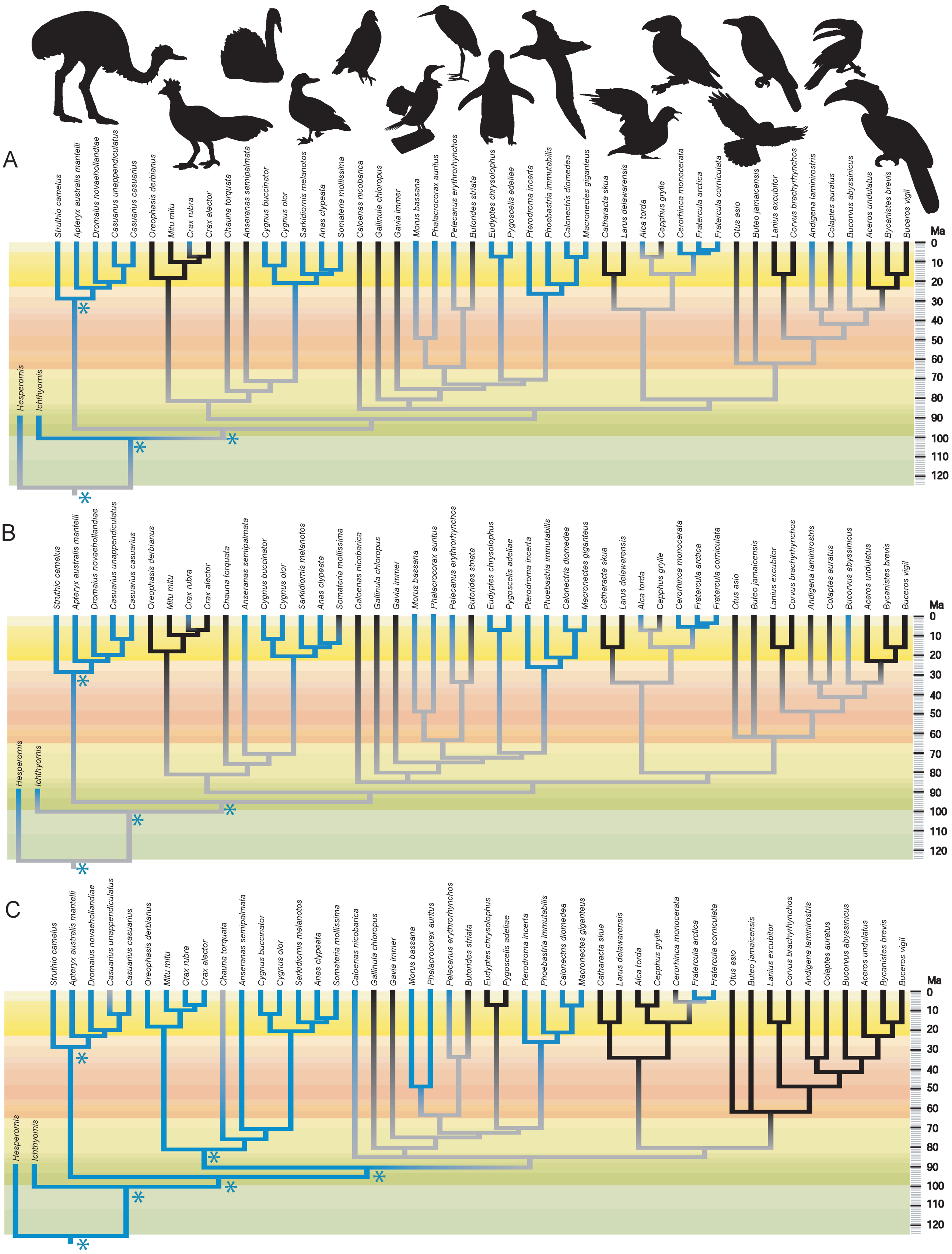
A
Struthio camelus
Apteryx australis mantelli
Dromaius novaehollandiae
Casuarius unappendiculatus
Casuarius casuarius
Oreophasis derbianus
Mitu mitu
Crax rubra
Crax alector
Chauna torquata
Anseranas semipalmata
Cygnus buccinator
Cygnus olor
Sarkidiornis melanotos
Anas clypeata
Somateria mollissima
Caloenas nicobarica
Gallinula chloropus
Gavia immer
Morus bassana
Phalacrocorax auritus
Pelecanus erythrorhynchos
Butorides striata
Eudyptes chrysolophus
Pygoscelis adeliae
Pterodroma incerta
Phoebastria immutabilis
Calonectris diomedea
Macronectes giganteus
Catharacta skua
Larus delawarensis
Alca torda
Cepphus grylle
Cerorhinca monocerata
Fratercula arctica
Fratercula corniculata
Otus asio
Buteo jamaicensis
Lanius excubitor
Corvus brachyrhynchos
Andigena laminirostris
Colaptes auratus
Bucorvus abyssinicus
Aceros undulatus
Bycanistes brevis
Buceros vigil
Hesperornis
Ichthyornis
Ma
0
10
20
30
40
50
60
70
80
90
100
110
120
B
Struthio camelus
Apteryx australis mantelli
Dromaius novaehollandiae
Casuarius unappendiculatus
Casuarius casuarius
Oreophasis derbianus
Mitu mitu
Crax rubra
Crax alector
Chauna torquata
Anseranas semipalmata
Cygnus buccinator
Cygnus olor
Sarkidiornis melanotos
Anas clypeata
Somateria mollissima
Caloenas nicobarica
Gallinula chloropus
Gavia immer
Morus bassana
Phalacrocorax auritus
Pelecanus erythrorhynchos
Butorides striata
Eudyptes chrysolophus
Pygoscelis adeliae
Pterodroma incerta
Phoebastria immutabilis
Calonectris diomedea
Macronectes giganteus
Catharacta skua
Larus delawarensis
Alca torda
Cepphus grylle
Cerorhinca monocerata
Fratercula arctica
Fratercula corniculata
Otus asio
Buteo jamaicensis
Lanius excubitor
Corvus brachyrhynchos
Andigena laminirostris
Colaptes auratus
Bucorvus abyssinicus
Aceros undulatus
Bycanistes brevis
Buceros vigil
Hesperornis
Ichthyornis
Ma
0
10
20
30
40
50
60
70
80
90
100
110
120
C
Struthio camelus
Apteryx australis mantelli
Dromaius novaehollandiae
Casuarius unappendiculatus
Casuarius casuarius
Oreophasis derbianus
Mitu mitu
Crax rubra
Crax alector
Chauna torquata
Anseranas semipalmata
Cygnus buccinator
Cygnus olor
Sarkidiornis melanotos
Anas clypeata
Somateria mollissima
Caloenas nicobarica
Gallinula chloropus
Gavia immer
Morus bassana
Phalacrocorax auritus
Pelecanus erythrorhynchos
Butorides striata
Eudyptes chrysolophus
Pygoscelis adeliae
Pterodroma incerta
Phoebastria immutabilis
Calonectris diomedea
Macronectes giganteus
Catharacta skua
Larus delawarensis
Alca torda
Cepphus grylle
Cerorhinca monocerata
Fratercula arctica
Fratercula corniculata
Otus asio
Buteo jamaicensis
Lanius excubitor
Corvus brachyrhynchos
Andigena laminirostris
Colaptes auratus
Bucorvus abyssinicus
Aceros undulatus
Bycanistes brevis
Buceros vigil
Hesperornis
Ichthyornis
Ma
0
10
20
30
40
50
60
70
80
90
100
110
120

Table 1. Likelihood ratios (expressed as present:absent) and maximum-parsimony ancestral-character-state reconstructions for presence–absence of rhamphothecal grooves at clades shown in Figure 4. Superscripts indicate the phylogenetic hypothesis used in reconstruction (E: Ericson et al. 2006; L: Livezey and Zusi 2007; H: Hackett et al. 2008). *Hesperornis* and *Ichthyornis* emerge as sister taxa in the phylogenetic hypothesis of Livezey and Zusi (2007), resulting in the absence of the clade Carinatae and reduced support for the congruence of nasolabial and culminolabial grooves in Neornithes and neognathous birds. Phylogenetic analyses that include other basal ornithurine birds, albeit with less extensive data matrices (e.g., Chiappe 2002, You et al. 2006), generally place *Ichthyornis* as closer to neornithine birds than *Hesperornis* in a monophyletic Carinatae. Asterisks indicate significance of maximum-likelihood ancestral-character-state reconstruction at $P \leq 0.05$. A = absent by maximum-parsimony reconstruction; P = present by maximum-parsimony reconstruction; a dash indicates equivocality.

Clade name	Nasolabial groove	Culminolabial groove	Mentolabial groove	Infralabial groove
Ornithurae^{H}	5.81 / P	2.90 / P	53.0* / P	— / A
Ornithurae^{E}	5.14 / P	2.21 / P	68.7* / P	— / A
Ornithurae^{L}	2.93 / P	2.12 / P	26.5* / P	— / A
Carinatae^{H}	8.92* / P	5.41 / P	431* / P	— / A
Carinatae^{E}	7.64* / P	4.38 / P	673* / P	— / A
Neornithes^{H}	4.78 / P	3.34 / P	176* / P	0.24 / A
Neornithes^{E}	4.13 / P	2.84 / P	258* / P	0.39 / A
Neornithes^{L}	1.20 / P	1.07 / P	19.1* / P	0.25 / A
Palaeognathae^{H}	50.7* / P	15.3* / P	1010* / P	0.34 / A
Palaeognathae^{E}	39.9* / P	7.97* / P	1460* / P	0.39 / A
Palaeognathae^{L}	3.81 / P	2.08 / P	61.9* / P	0.27 / A
Neognathae^{H}	2.58 / A	2.23 / A	57.9* / P	0.25 / A
Neognathae^{E}	2.26 / A	2.03 / –	76.0* / P	0.39 / A
Neognathae^{L}	0.88 / A	0.91 / A	12.8* / P	0.25 / A
Galloanserae^{H}	1.65 / A	1.76 / A	135* / P	0.28 / A
Galloanserae^{E}	1.52 / A	1.59 / –	204* / P	0.39 / A
Galloanserae^{L}	0.72 / A	0.95 / A	12.8* / P	0.30 / A
Neoaves^{H}	1.92 / A	1.57 / A	4.01 / –	0.23 / A
Neoaves^{E}	1.91 / A	1.74 / –	8.79 / P	0.39 / A
Neoaves^{L}	0.81 / A	0.83 / A	2.73 / A	0.24 / A

latericorn or, instead, the existing latericorn extended onto the jugal bar and subsequently divided to accommodate kinesis about the jugal hinge. The relative likelihood of these scenarios cannot be established without a better understanding of the mechanisms that define the caudal boundary of the upper rhamphotheca during development.

Parts of the compound rhamphotheca are primitive for Neornithes.—The basal ornithurine birds *Hesperornis* and *Ichthyornis* show clear osteological correlates for both nasolabial and mentolabial grooves. The presence of these features in basal Ornithurae and Palaeognathae leads to an unambiguous MP ancestral-character-state reconstruction of these components of the compound rhamphotheca as primitive for Neornithes (Fig. 4). The ML reconstructions are somewhat more varied, unambiguously supporting the mentolabial groove as the primitive state for Neornithes and Neognathae but showing only marginal ML support ($p < 0.2$) for the nasolabial groove as the primitive state for Neornithes (Table 1). Thus, compound rhamphothecae in a broad sense in basal ornithurine birds (Odontoholomorphae and Palaeognathae) easily pass Patterson's (1982) congruence test of homology, and congruence of these structures into Neognathae and the base of Galloanserae is likely as well (Fig. 4).

The base of Neoaves shows likelihood ratios that are skewed in favor of the presence of mentolabial, culminolabial, and/or nasolabial grooves, but this falls short of statistical significance. This ambiguity prevents a straightforward assessment of congruence for the compound rhamphothecae observed in Pelecaniformes, Procellariiformes, and Sphenisciformes. The most likely interpretation is that these examples of compound rhamphothecae are congruent with the primitive state observed in palaeognaths, but the alternative hypothesis that they are convergent structures cannot be entirely discounted with the available data. Compound rhamphothecae in these neoavian taxa thus conditionally pass the congruence test of Patterson (1982), but their marked similarity to compound rhamphothecae in palaeognaths may also be attributable to similarity in development or syngeny.

The examples of prominent mentolabial, culminolabial, and nasolabial grooves seen in other neoavians, such as Great Skuas and several alcids (*Fratercula* spp., Rhinoceros Auklet), are more likely to be instances of convergence than the retention of primitive compound rhamphothecae. Although these examples are not congruent, they still pass the similarity and nonconjunction tests of Patterson (1982), which suggests that they may be the result of similar processes in development.

The remaining examples of rhamphothecal grooves within Coraciiformes and Piciformes are also not congruent, but in some cases they retain strong similarity to grooves in the primitive compound rhamphothecae of Neornithes. Many Piciformes (e.g., Northern Flicker) bear a shallow nasolabial groove (Fig. 2G). This feature may be related to nasolabial grooves in other avian taxa in the same manner as the rhamphothecal grooves in alcids: not homologous, but possibly derived from similar development. Other examples of rhamphothecal grooves in Coraciiformes and Piciformes, such as the grooves between lateral and rostral parts of the maxillary rhamphotheca in *Bucorvus* spp. and Plate-billed Mountain-Toucan, show only superficial similarity with the nasolabial grooves of basal Neornithes.

Some "compound" elements are independently derived within Neornithes.—The congruent state for rhamphothecae in basal neornithines involves some, but not all, of the separate plates seen in extant birds. The basal neornithine state shows a shallow culminolabial groove between premaxillary nail and culminicorn. Both of these plates are separated from the latericorns by a prominent nasolabial groove. Skin surrounding the nostril is less cornified than the adjacent beak plates, and thus a naricorn, as seen in Procellariiformes, is absent. The mandibular rhamphotheca is divided by a mentolabial groove into a mandibular nail and a single ramicorn on each side, but an infralabial groove is absent.

Whereas the culminolabial, nasolabial, and mentolabial grooves are primitive for Neornithes, a number of other elements of compound rhamphothecae appear to be independently derived in various neornithine clades. The separate, heavily cornified naricorns that have led to the name "tubenoses" for procellariiform seabirds are an apomorphy of the (Gaviiformes + [Pelecaniformes + Ciconiiformes] + [Sphenisciformes + Procellariiformes]) clade of Hackett et al. (2008; Fig. 4) and are derived from an area of relatively soft, cereous skin that surrounds the nostril in palaeognaths and galloanserine birds. A separate naricorn is absent in most of the derived "ground birds" and charadriiforms, although the margin of the nostril is generally cornified in these taxa, in contrast to the softer cereous skin seen in palaeognaths and galloanserines.

An infralabial groove is derived independently in Anatoidea, some Procellariiformes, and *Casuarius* spp. This feature is similar in topology to the infralabial notch present in palaeognaths and some galloanserine birds but does not appear to be primitive for Neornithes. In anatoids and procellariiforms, the infralabial groove accompanies a series of foramina from the mandibular canal. The gross and histological relationships of the nerves and vessels that pass though these foramina are not well understood, but it is possible that the infralabial groove presents a thin-walled area of rhamphotheca allowing for more sensitive mechanoreception along the lateral surface of the mandible.

A pseudomental fold occurs independently in Procellariiformes and steganopode pelecaniforms but is absent in their commonly recognized closest relatives Ciconiiformes, Sphenisciformes, and Gaviiformes. The pseudomental folds of steganopode pelecaniforms and Procellariiformes both cover a thin bony strut that projects caudally from the mandibular symphysis. The factors that contribute to the strong similarity between these convergent morphologies are unknown.

Revised hypothesis of homology for avian rhamphotheca.—Our findings of (1) strong morphological similarity between diverse examples of compound rhamphothecae, (2) congruence of similar rhamphothecal morphologies at the base of Neornithes, and (3) persistent relationships between rhamphothecal morphology and underlying bone and nerve structures all lead to a revised hypothesis of homology between areas of rhamphothecae in Neornithes (Fig. 5). This hypothesis covers rhamphothecal plates found to be primitive for Neornithes, but not plates that are autapomorphic for individual neornithine clades (e.g., the dorsal and ventral ramicorns of Southern Giant Petrel). Transition to a simple rhamphotheca occurs with the loss of rhamphothecal grooves, but similarity in the topological relationships of areas of rhamphotheca are retained (Fig. 5B). The remaining caudal portions of simple upper rhamphothecae show a topological relationship to the underlying maxillary process of the premaxilla and branches of the nasopalatine nerve that is nearly identical to that seen in compound upper rhamphothecae. These persistent topological relationships would not be expected if simple rhamphothecae arose instead by the loss of the caudal plates of compound rhamphothecae.

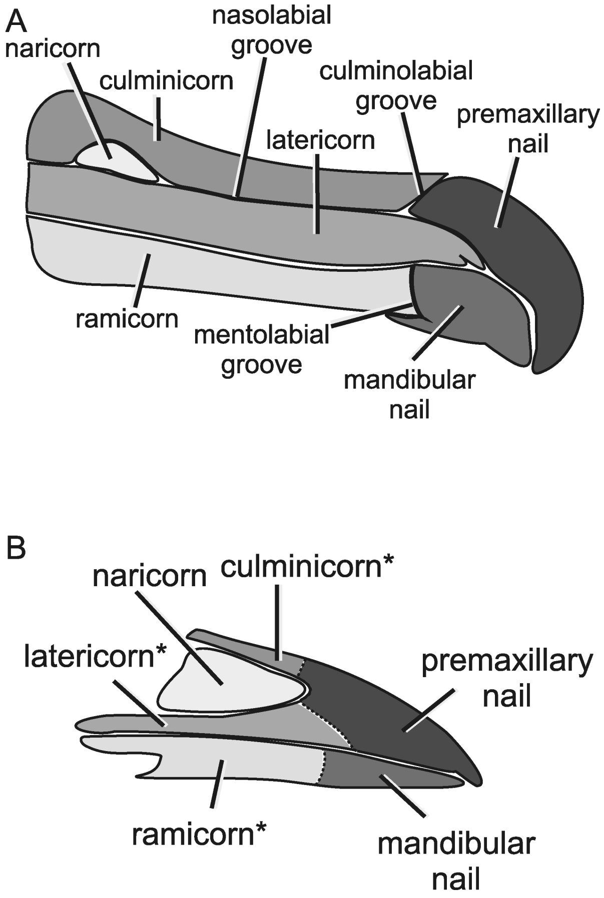

Fig. 5. Hypothesis of homology for areas of rhamphothecae proposed in the present study, shown on (A) Laysan Albatross and (B) American Crow. Regions marked by asterisks in B are fused with other plates that share a common direction of growth and are delineated on the basis of topological relationships to underlying bones and nerves.

Our hypothesis differs from that of Lönnberg (1904) in two important respects. (1) Several of the components shown in Figure 1B are subsumed into single elements. The first and second supralabials are combined into a single latericorn, the mental and first infralabial are combined into a single mental, and the second infralabial and submandibular are combined into a single ramicorn.

(2) The conceptual positions of plate "fusion" to form simple rhamphothecae are more rostrally positioned in the revised hypothesis. Our revision differs from the hypothesis of von Boetticher (1928) in considering upper and lower simple rhamphothecae to be directly comparable to the entire compound rhamphotheca, not only the rostral and the mental portrayed in Figure 1D. The character polarizations shown in Figure 4 also place compound rhamphothecae as primitive for Ornithurae, reversing von Boetticher's (1928) assessment of simple rhamphothecae as the primitive state for bird beaks.

Discussion

Evolution of rhamphothecal morphology within Neornithes.—A scenario for the evolutionary history of compound rhamphothecae in neornithine clades can be briefly summarized as a series of trends, with the acknowledgment that the data set presented here can provide only a rough sketch. For example, palaeognaths largely retain the primitive arrangement of plates and grooves in their compound rhamphothecae, but in comparison to *Ichthyornis* and *Hesperornis*, the size of the premaxillary and mandibular nails in relation to the rest of the rostrum has been reduced. Reduction of the premaxillary and mandibular nails results in a predominantly rostrocaudal orientation of the nasolabial and mentolabial grooves.

Galloanserine birds show a general reduction of the nasolabial groove, with some atavistic exceptions (e.g., Great Curassow). The culminolabial groove remains shallow or is lost in most galliform birds but is exaggerated in many anatoids, such that the division between the premaxillary nail and the rest of the upper rhamphotheca is the most pronounced anatomical feature of the skin of the upper beak. Despite this trend at the base of Anatidae, the culminolabial groove is secondarily reduced in some anseriform taxa (e.g., *Somateria*). The mentolabial groove is reduced in galliform birds and is marked only by the transition from relatively soft skin covering the mandibular rami to cornified skin across the mandibular symphysis. The anatoid mentolabial groove is retained and in some cases exaggerated, resulting in a distinct mandibular nail that matches the premaxillary nail.

Neoavians show a trend of increasing cornification of the culminicorn and naricorns. Some neoavian clades (e.g., Columbiformes in the topology of Hackett et al. 2008) retain a soft, cereous skin in these areas, and it is unclear whether this morphology constitutes a reversal from a cornified state or, rather, cornification of the culminicorn and naricorns occurred several times.

Several neoavian clades also show a trend toward a simple conical or crescentic bony rostrum, in contrast to the more complex shapes seen in ratites and procellariiform birds. This contrast can be seen most clearly in comparing closely related taxa such as cormorants (*Phalacrocorax* spp.) and darters (*Anhinga* spp.). Cormorants retain a saddle-shaped culminicorn and a separate, sickle-shaped premaxillary nail on a boxy, bony rostrum, while also retaining pronounced nasolabial and culminolabial grooves. Darters, on the other hand, show a fused culminicorn and premaxillary nail on a conical bony rostrum, with the nasolabial groove retained only as a shallow fold.

Groove function in compound rhamphothecae.—Plates of compound rhamphothecae exhibit different directions of apparent growth. Most plates that make up part of the maxillary and mandibular tomia show a tendency to translate across the surface of the bony rostrum and dermis toward the tomia, rather than growing perpendicular to the surface of the dermis (Fig. 6). The cornified epidermis of the rhamphotheca is stiff (Bonser and Witter 1993) and will accommodate only relatively small strains and deformation during growth (Lüdicke 1933). Although individual plates show clear boundaries of cornification, with softer grooves intervening, the germinative layer of epidermal cells that underlies these structures is continuous across the entire rostrum. Less cornified grooves between plates may allow the softer skin in the groove to deform as a single generation of epithelial cells begins to grow in different directions. As the less cornified epidermis of the groove breaks down and wears away, the links between separate plates are lost, allowing the heavily cornified plates to continue in their direction of growth as independent units (Fig. 6). Loss of the softer grooves in a compound rhamphotheca to form a simple rhamphotheca may depend on whether the bony rostrum forms a consistent cross-sectional shape that allows the entire rhamphotheca to translate across its surface as a single unit during growth (Lüdicke 1933).

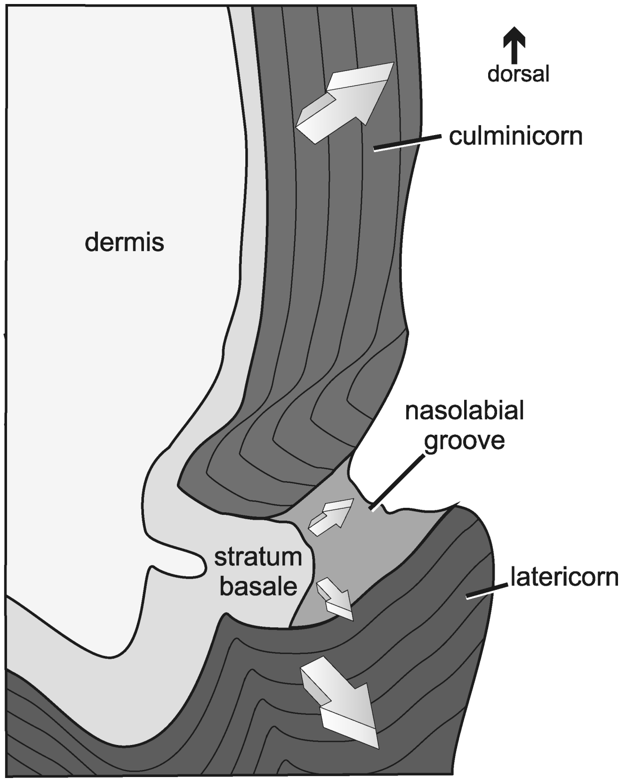

Fig. 6. Schematic cross section of the nasolabial groove, illustrating the possible function of rhamphothecal grooves in growth and maintenance of adult rhamphothecal shape, drawn from a histological section of a Double-crested Cormorant, OUVC 10401). White arrows indicate the direction of growth of the culminicorn and latericorn, including growth out of the plane of the section. The strain that results from cornified plates growing in different directions may be taken up by the softer, less cornified tissue in the nasolabial groove, which would wear and fall apart more quickly than the surrounding cornified plates.

Potential underlying similarity in compound rhamphothecae.—The frequent reversal to compound rhamphothecae among neoavians suggests an underlying similarity in beak development. Some elements of this idea have previously been suggested by Olson (1985), who pointed to histological descriptions of "labial grooves" (corresponding to the nasolabial and mentolabial grooves) in developing chickens (Kingsbury et al. 1953).

The hypothesis that the "labial grooves" of developing chickens are transitory homologs to rhamphothecal grooves in palaeognaths is in accord with other sources of data on rhamphothecal development. Nasolabial and mentolabial grooves develop in *Gallus* and other birds in the early stages of rhamphothecal keratinization (embryonic day [ED] 10, Hamburger and Hamilton stage [HH] 36; Hamburger and Hamilton 1951) and are lost in *Gallus* by ED 17 (HH 43), whereas they remain prominent in *Larus* and *Columba* (Bartels and Flachsbarth 1994). There is also some correspondence between parts of the compound rhamphotheca and the initial development of centers of ossification in the rostrum. The nasolabial groove corresponds to the initial position of the premaxillomaxillary suture before the subnarial bar of the premaxilla develops (Jollie 1957, Bartels and Flachsbarth 1994). Similarly, the mentolabial groove corresponds to the separation between the mentomeckelian (mentomandibular, predentary) ossification and the more caudal ossification of the dentaries (Jollie 1957) before these centers fuse in later development. It is unclear whether a causal relationship exists between centers of ossification in the rostrum and areas of cornified skin in compound rhamphothecae, but the similar topology of these structures raises the possibility that both are related as an "underlying synapomorphy" or syngeny that may explain the homoplastic occurrence of rhamphothecal grooves in Charadriiformes, Coraciiformes, and Piciformes.

"Egg teeth" and rhamphothecal evolution.—Avian "egg teeth" are transitory thickened and calcified areas of skin that develop on the tip of the rostrum during the early stages of skin keratinization. Other terms for these structures (Eischwielen, caruncles) reflect their epidermal origin and distinguish them from the dentinous egg teeth (Eizähne) found in squamates (Röse 1892). Caruncles are a synapomorphy of amniotes, present in monotremes (Hughes and Hall 1998), turtles (Miller 1985), and crocodylians (Ferguson 1985) in addition to birds, and absent only in therian mammals and squamates. On the basis of the phylogenetic distribution of beaked forms in the fossil record and the congruence of that pattern with the presence or absence of a caruncle, Lee (1997) suggested that the multiple independent origins of rhamphothecae (in birds, turtles, and at least 13 extinct amniote lineages) are all derived from elaborations of caruncles. The possible role of caruncles in rhamphothecal evolution in the lineage leading to neornithine birds can be evaluated using additional information.

Caruncles in *Gallus* begin to cornify somewhat earlier than the subjacent rhamphothecae (Kingsbury et al. 1953, Tonégawa 1973). The caruncle forms the initial center of rhamphothecal keratinization, which then spreads gradually across the surface of the rostrum (Kingsbury et al. 1953). Several avian taxa have been reported to bear caruncles on both the premaxillary nail and the mandibular nail (Clark 1961) in a phylogenetic distribution that ranges from Galloanserae (*Gallus*), through Metaves (several Columbidae), basal Coronaves (*Gavia*, *Gallinula*), Charadriiformes (*Burhinus*, *Haematopus*, *Chlidonias*), Falconiformes (*Milvus*), Piciformes and Coraciiformes (*Buceros*, *Colaptes*), to Passeriformes (*Turdus*, *Agelaius*). The broad distribution of this trait suggests that the presence of a caruncle on both the premaxillary nail and the mandibular nail may be plesiomorphic for Neornithes. These data are not enough, by themselves, to fully test whether avian rhamphothecae are an exaptation or iterative homolog of the caruncle, but the origin of avian rhamphotheca as a derivative of the upper and lower caruncles currently stands as the best available hypothesis for rhamphothecal evolution in neornithine birds.

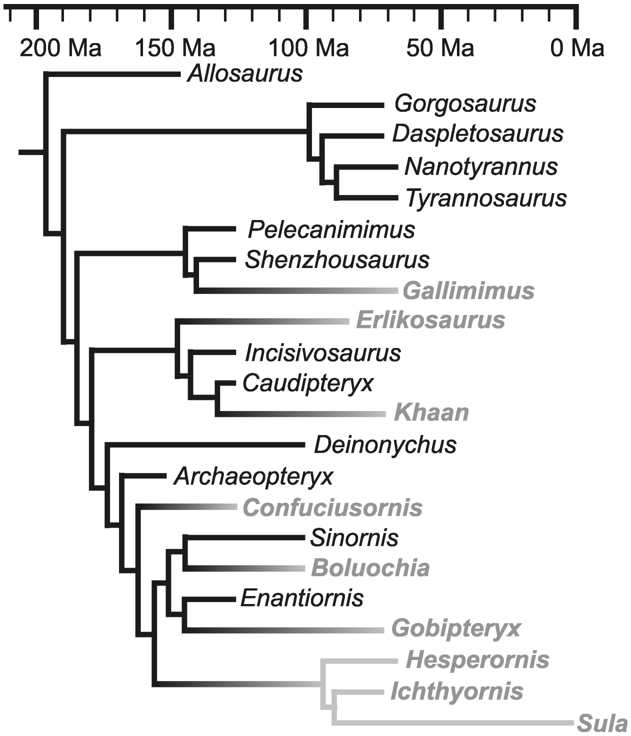

Fig. 7. Representative phylogeny of derived coelurosaurian dinosaurs, showing the mosaic evolution of rhamphothecae within this clade (gray branches and genus names). The density of convergent occurrences of rhamphothecae in Coelurosauria stands in contrast to the relative rarity of the evolution of similar structures in other amniotes. Topology after Chiappe (2002), Holtz (2004), Holtz et al. (2004), Makovicky et al. (2004), and Osmólska et al. (2004).

Compound rhamphothecae as defined by the nasolabial, culminolabial, and mentolabial grooves are a primitive trait for neornithine birds and are a synapomorphy of the more inclusive clade (Odontoholomorphae + Neornithes, in the sense of Livezey and Zusi 2007). In basal members of this clade such as *Hesperornis* and *Ichthyornis*, the premaxillary and mandibular nails appear to have been the most heavily cornified parts of the rhamphotheca. The presence of true teeth in the maxillae and dentaries of *Ichthyornis* and *Hesperornis* suggests that tomia may not have been present on the latericorn and ramicorn in these taxa and that complete tomia on the dorsal and ventral oral margins are a synapomorphy of Neornithes.

Extensive cornification of the naricorn and culminicorn appears to be a recurring trend within Neoaves. The pronounced compound rhamphothecae present in neoavians such as Procellariiformes and Pelecaniformes most likely reflect the evolution of heavy cornification across the entire rhamphotheca before the evolution of a morphologically simple bony rostrum, perhaps coupled with a function for the nasolabial groove as a gutter for draining the nasal salt glands. The evolution of a simple conical or crescentic bony rostrum occurs several times within Neornithes, and this morphology appears to be a prerequisite for the loss of rhamphothecal grooves and the transition to simple rhamphothecae.

The evolution of rhamphothecae in ornithurine birds represents only one of at least seven independent occurrences of rhamphothecae in coelurosaurian dinosaurs, all clustered within a span of 35 million years from the Late Jurassic through the Early Cretaceous (Fig. 7). This is a striking example of mosaic evolution. Outside of this closely related group of coelurosaurian dinosaurs, there is fossil evidence for only eight other independent occurrences of rhamphothecae in amniotes, and only one of those lineages (turtles) is still extant. Establishing the evolutionary history of rhamphothecae in neornithine birds provides a morphological context for addressing the mosaic evolution of similar structures within Coelurosauria. Comparisons of the morphology and development of avian rhamphothecae with the bony morphology of the rostrum in coelurosaurian dinosaurs may provide a window into the early evolution of one of the most characteristic features of modern birds.

Acknowledgments

Discussion and correspondence with L. Alibardi, L. N. Cooper, J. Daniel, D. Dufeau, C. Holliday, D. Homberger, A. Horner, J. Hutchinson, G. Mayr, E. McElroy, H. Maddin, P. Maderson, P. O'Connor, C. Organ, M. Rubega, N. Stevens, A. Stigall, and T. Tsuihiji have greatly aided this research. G. Mayr and two anonymous reviewers provided thoughtful comments on an earlier version of the manuscript. For access to histology and microscopy equipment, we thank D. Hembree, D. Kidder, G. Nadon, P. O'Connor, G. Rothwell, and S. Williams. D. Dufeau and R. Ridgely at OUμCT provided invaluable assistance with CT scanning. For access to osteological and paleontological specimens, we thank M. Peck at the Royal Ontario Museum, J. Hinshaw at the University of Michigan Museum of Zoology, S. Rogers at the Carnegie Museum of Natural History, P. Sweet at the American Museum of Natural History, and G. Mayr at the Naturmuseum Senckenberg. This research was funded by the Jurassic Foundation (T.L.H.), the National Science Foundation (NSF IBN-0343744 & IOB-0517257; L.M.W.), and Ohio University (T.L.H.). For information on the chronostratigraphic units proposed by the Commission for the Geological Map of the World, please visit ccgm.free.fr/index_gb.html.

Literature Cited

Bartels, T., and M. F. Flachsbarth. 1994. Rasterelektronenmikroskopische Untersuchungen zur Entwicklung des Vogelschnabels. Zoologischer Anzeiger 232:97–110.

Benton, M. J., and P. C. J. Donoghue. 2007. Paleontological evidence to date the tree of life. Molecular Biology and Evolution 24:26–53.

Bonser, R. H. C., and M. S. Witter. 1993. Indentation hardness of the bill keratin of the European Starling. Condor 95:736–738.

Butler, A. B., and W. M. Saidel. 2000. Defining sameness: Historical, biological, and generative homology. BioEssays 22: 846–853.

Chandler, A. C. 1916. A study of the structure of feathers, with reference to their taxonomic significance. University of California Publications in Zoology 13:243–446.

Chiappe, L. M. 2002. Basal bird phylogeny: Problems and solutions. Pages 448–472 *in* Mesozoic Birds: Above the Heads of Dinosaurs (L. M. Chiappe and L. M. Witmer, Eds.). University of California Press, Berkeley.

Clark, G. A., Jr. 1961. Occurrence and timing of egg teeth in birds. Wilson Bulletin 73:268–278.

Clarke, J. A. 2004. Morphology, phylogenetic taxonomy, and systematics of *Ichthyornis* and *Apatornis* (Avialae: Ornithurae). Bulletin of the American Museum of Natural History, no. 286.

Coues, E. 1866. Critical review of the family Procellariidae: Part V; embracing the Diomedeinae and the Halodrominae. With a general supplement. Proceedings of the Academy of Natural Sciences of Philadelphia 18:172–197.

Donne-Goussé, C., V. Laudet, and C. Hänni. 2002. A molecular phylogeny of Anseriformes based on mitochondrial DNA analysis. Molecular Phylogenetics and Evolution 23:339–356.

Elzanowksi, A. 1991. New observations on the skull of *Hesperornis* with reconstructions of the bony palate and otic regions. Postilla 207:1–20.

Ericson, P. G. P., C. L. Anderson, T. Britton, A. Elzanowski, U. S. Johansson, M. Källersjö, J. I. Ohlson, T. J. Parsons, D. Zuccon, and G. Mayr. 2006. Diversification of Neoaves: Integration of molecular sequence data and fossils. Biology Letters 2:543–547.

Ferguson, M. W. J. 1985. Reproductive biology and embryology of the crocodilians. Pages 329–492 *in* Biology of the Reptilia, vol. 14A (C. Gans, F. Billett, and P. F. A. Maderson, Eds.). Wiley, New York.

Gadow, H., and E. Selenka. 1891. Vogel. I. Anatomischer Theil. Pages 1–1008 *in* Bronn's Klassen und Ordnungen des Thier-Reichs, vol. 6 (H. G. Bronn, Ed.). C. F. Winter, Leipzig, Germany.

Hackett, S. J., R. T. Kimball, S. Reddy, R. C. K. Bowie, E. L. Braun, M. J. Braun, J. L. Chojnowski, W. A. Cox, K.-L. Han, J. Harshman, and others. 2008. A phylogenomic study of birds reveals their evolutionary history. Science 320:1763–1768.

Hall, B. K. 2003. Descent with modification: The unity underlying homology and homoplasy as seen through an analysis of development and evolution. Biological Reviews 78:409–433.

Hamburger, V., and H. L. Hamilton. 1951. A series of normal stages in the development of the chick embryo. Journal of Morphology 88:49–92.

Holtz, T. R., Jr. 2004. Tyrannosauroidea. Pages 111–136 *in* The Dinosauria (D. B. Weishampel, P. Dodson, and H. Osmólska, Eds.). University of California Press, Berkeley.

Holtz, T. R., Jr., R. E. Molnar, and P. J. Currie. 2004. Basal Tetanurae. Pages 71–110 *in* The Dinosauria (D. B. Weishampel, P. Dodson, and H. Osmólska, Eds.). University of California Press, Berkeley.

Hughes, R. L., and L. S. Hall. 1998. Early development and embryology of the platypus. Philosophical Transactions of the Royal Society of London, Series B 353:1101–1114.

Jollie, M. T. 1957. The head skeleton of the chicken and remarks on the anatomy of this region in other birds. Journal of Morphology 100:389–436.

Kemp, A. C. 1988. The systematics and zoogeography of Oriental and Australasian hornbills (Aves: Bucerotidae). Bonner Zoologische Beiträge 39:315–345.

Kennedy, M., and R. D. M. Page. 2002. Seabird supertrees: Combining partial estimates of procellariiform phylogeny. Auk 119: 88–108.

Kingsbury, J. W., V. G. Allen, and B. A. Rotheram. 1953. The histological structure of the beak in the chick. Anatomical Record 116:95–115.

Lee, M. S. Y. 1997. The evolution of beaks in reptiles: A proposed evolutionary constraint. Evolutionary Theory and Review 11:249–254.

Livezey, B. C. 1996. A phylogenetic analysis of geese and swans (Anseriformes: Anserinae), including selected fossil species. Systematic Biology 45:415–450.

Livezey, B. C. 1997. A phylogenetic analysis of basal Anseriformes, the fossil *Presbyornis*, and the interordinal relationships of waterfowl. Zoological Journal of the Linnean Society 121:361–428.

Livezey, B. C., and R. L. Zusi. 2006. Higher-order phylogeny of modern birds (Theropoda, Aves: Neornithes) based on comparative anatomy. I. Methods and characters. Bulletin of the Carnegie Museum of Natural History, no. 37.

Livezey, B. C., and R. L. Zusi. 2007. Higher-order phylogeny of modern birds (Theropoda, Aves: Neornithes) based on comparative anatomy. II. Analysis and discussion. Zoological Journal of the Linnean Society 149:1–95.

Lönnberg, E. 1904. On the homologies of the different pieces of the compound rhamphotheca of birds. Arkiv für Zoologie 1:479–512.

Lüdicke, M. 1933. Wachstum und Abnutzung des Vogelschnabels. Zoologische Jahrbücher, Abteilung für Anatomie und Ontogenie der Tiere 57:435–564.

MacDonald, J. D. 1960. Secondary external nares of the gannet. Proceedings of the Zoological Society of London 135:357–363.

Maddison, W. P., M. J. Donoghue, and D. R. Maddison. 1984. Outgroup analysis and parsimony. Systematic Zoology 33:83–103.

Maddison, W. P., and D. R. Maddison. 2009. MESQUITE: A modular system for evolutionary analysis, version 2.71. [Online.] Available at mesquiteproject.org.

Makovicky, P. J., Y. Kobayashi, and P. J. Currie. 2004. Ornithomimosauria. Pages 137–150 *in* The Dinosauria (D. B. Weishampel, P. Dodson, and H. Osmólska, Eds.). University of California Press, Berkeley.

Martin, L. D. 1984. A new hesperornithid and the relationships of the Mesozoic birds. Transactions of the Kansas Academy of Science 87:141–150.

Martin, L. D. 1987. The beginning of the modern avian radiation. Documents des Laboratoires de Géologie de Lyon 99:9–19.

Miller, J. D. 1985. Embryology of marine turtles. Pages 269–328 *in* Biology of the Reptilia, vol. 14A (C. Gans, F. Billett, and P. F. A. Maderson, Eds.). Wiley, New York.

Olson, S. L. 1985. The fossil record of birds. Pages 79–252 *in* Avian Biology, vol. 8 (D. S. Farner, J. R. King, and K. C. Parkes, Eds.). Academic Press, New York.

Osmólska, H., P. J. Currie, and R. Barsbold. 2004. Oviraptorosauria. Pages 165–183 *in* The Dinosauria (D. B. Weishampel, P. Dodson, and H. Osmólska, Eds.). University of California Press, Berkeley.

Pagel, M. 1992. A method for the analysis of comparative data. Journal of Theoretical Biology 156:431–442.

Parkes, K. C., and G. A. Clark. 1966. An additional character linking ratites and tinamous, and an interpretation of their monophyly. Condor 68:459–471.

Patterson, C. 1982. Morphological characters and homology. Pages 21–74 *in* Problems of Phylogenetic Reconstruction (K. A. Joysey, and A. E. Friday, Eds.). Academic Press, London.

Pereira, S. L., and A. J. Baker. 2004. Vicariant speciation of curassows (Aves, Cracidae): A hypothesis based on mitochondrial DNA phylogeny. Auk 121:682–694.

Pereira, S. L., A. J. Baker, and A. Wajntal. 2002. Combined nuclear and mitochondrial DNA sequences resolve generic relationships within the Cracidae (Galliformes, Aves). Systematic Biology 51:946–958.

Remane, A. 1955. Morphologie als Homologienforschung. Verhandlungen der Deutschen zoologischen Gesellschaft 1954:159–183.

Remane, J. 1983. The concept of homology in phylogenetic research—Its meaning and possible applications. Paläontologische Zeitschrift 57:267–269.

Röse, C. 1892. Über die Zahnleiste und die Eischwiele der Sauropsiden. Anatomischer Anzeiger 7:748–758.

Roth, V. L. 1991. Homology and hierarchies: Problems solved and unresolved. Journal of Evolutionary Biology 4:167–194.

Sæther, O. A. 1979. Underlying synapomorphies and anagenetic analysis. Zoologica Scripta 8:305–312.

Schmidt-Nielsen, K., and R. Fänge. 1958. Salt glands in marine reptiles. Nature 182:783–785.

Schluter, D., T. Price, A. Ø. Mooers, and D. Ludwig. 1997. Likelihood of ancestor states in adaptive radiation. Evolution 51:1699–1711.

Sterchi, D. L., and J. A. Eurell. 1989. A new method for preparation of undecalcified bone sections. Stain Technology 64:201–205.

Storer, R. W. 1960. Adaptive radiation in birds. Pages 15–55 *in* Biology and Comparative Physiology of Birds, vol. 1 (A. J. Marshall, Ed.). Academic Press, New York.

Thomas, G. H., M. A. Wills, and T. Székely. 2004. A supertree approach to shorebird phylogeny. BMC Evolutionary Biology 4:28.

Tonégawa, Y. 1973. Inductive tissue interactions in the beak of a chick embryo. Development, Growth & Differentiation 15:57–71.

von Boetticher, H. 1928. Beitrag zur Kenntnis der Morphologie und Phylogenie des hornigen Vogelschnabelüberzuges mit besonderer Berücksichtigung seiner Beziehungen zu den Schnauzenschildern der Saurier. G. Fischer, Jena, Germany.

You, H., M. C. Lamanna, J. D. Harris, L. M. Chiappe, J. O'Connor, S. Ji, J. Lü, C. Yuan, D. Li, X. Zhang, K. J. Lacovara, P. Dodson, and Q. Ji. 2006. A nearly modern amphibious bird from the Early Cretaceous of northwestern China. Science 312:1640–1643.

Associate Editor: G. Mayr

APPENDIX. Taxa included in the present study. Taxa in bold were included in ancestral-character-state reconstructions. Material examined is coded as follows: O = osteological material; S = study skin (whole or partial preservation); F = fresh, frozen, or formalin-fixed; µCT = MicroCT scanned; VI = MicroCT with vascular injection; and H = histological preparation of rhamphotheca.

Taxon	Material examined
Wreathed Hornbill (*Aceros undulatus*)	O, S
Crested Auklet (*Aethia cristatella*)	S
Razorbill (*Alca torda*)	O, S
Northern Shoveler (*Anas clypeata*)	O, F, VI
African Openbill (*Anastomus lamelligerus*)	O, S
Plate-billed Mountain-Toucan (*Andigena laminirostris*)	S
Horned Screamer (*Anhima cornuta*)	O
Indian Darter (*Anhinga melanogaster*)	O
Magpie Goose (*Anseranas semipalmata*)	O, S
Indian Pied Hornbill (*Anthracoceros malabaricus*)	O
Emperor Penguin (*Aptenodytes forsteri*)	O
Brown Kiwi (*Apteryx australis*)	O, S
Little Spotted Kiwi (*A. owenii*)	O
Limpkin (*Aramus guarauna*)	O
Gray Heron (*Ardea cinerea*)	O
Kori Bustard (*Ardeotis kori*)	O
Great Argus (*Argusianus argus*)	O
Shoebill (*Balaeniceps rex*)	O
Great Hornbill (*Buceros bicornis*)	O
Rufous Hornbill (*B. hydrocorax*)	O
Helmeted Hornbill (*B. vigil*)	O, S
Northern Ground Hornbill (*Bucorvus abyssinicus*)	O, S
Southern Ground Hornbill (*B. leadbetteri*)	O
Red-tailed Hawk (*Buteo jamaicensis*)	O, F, µCT
Striated Heron (*Butorides striata*)	O, F, µCT
Silvery-cheeked Hornbill (*Bycanistes brevis*)	O, S
Trumpeter Hornbill (*B. bucinator*)	O
Nicobar Pigeon (*Caloenas nicobarica*)	O, S
Cory's Shearwater (*Calonectris diomedea*)	O, S
Southern Cassowary (*Casuarius casuarius*)	O, S
Northern Cassowary (*C. unappendiculatus*)	O, S
Great Skua (*Catharacta skua*)	O, S
Black Guillemot (*Cepphus grylle*)	O
Piping Hornbill (*Ceratogymna fistulator*)	O
Rhinoceros Auklet (*Cerorhinca monocerata*)	O, S
Southern Screamer (*Chauna torquata*)	O, S
Snowy Sheathbill (*Chionis alba*)	O
Northern Flicker (*Colaptes auratus*)	O, F, VI, H
American Crow (*Corvus brachyrhynchos*)	O, F, VI, H
Black Curassow (*Crax alector*)	O, S
Great Curassow (*C. rubra*)	O, S
Trumpeter Swan (*Cygnus buccinator*)	O, F
Mute Swan (*C. olor*)	O, S
Cape Petrel (*Daption capense*)	O
Tooth-billed Pigeon (*Didunculus strigirostris*)	S
Antipodean Albatross (*Diomedea antipodensis*)	O
Black-browed Albatross (*D. melanophris*)	O
Emu (*Dromaius novaehollandiae*)	O, F
Pileated Woodpecker (*Dryocopus pileatus*)	O
Little Egret (*Egretta garzetta*)	O
Macaroni Penguin (*Eudyptes chrysolophus*)	O, S
Little Penguin (*Eudyptula minor*)	O
Sunbittern (*Eurypyga helias*)	O
Gyrfalcon (*Falco rusticolus*)	O
Atlantic Puffin (*Fratercula arctica*)	O, S
Tufted Puffin (*F. cirrhata*)	O, S
Horned Puffin (*F. corniculata*)	O, S
Great Frigatebird (*Fregata minor*)	O
Fregata sp.	O
Northern Fulmar (*Fulmarus glacialis*)	O
Common Moorhen (*Gallinula chloropus*)	O, F, µCT
Common Loon (*Gavia immer*)	O, F, VI
Red-throated Loon (*G. stellata*)	O
Blue Petrel (*Halobaena caerulea*)	O
Northern Shrike (*Lanius excubitor*)	O, S
Herring Gull (*Larus argentatus*)	O
Ring-billed Gull (*L. delawarensis*)	O, F, VI, H
Hooded Merganser (*Lophodytes cucullatus*)	O
Southern Giant Petrel (*Macronectes giganteus*)	O, S
Macronectes sp.	O
Pink-eared Duck (*Malacorhynchus membranaceus*)	O
Common Merganser (*Mergus merganser*)	O
Alagoas Curassow (*Mitu mitu*)	S
Northern Gannet (*Morus bassanus*)	O, F
Great Potoo (*Nyctibius grandis*)	O
Wilson's Storm-Petrel (*Oceanites oceanicus*)	O
Horned Guan (*Oreophasis derbianus*)	S
Eastern Screech-Owl (*Megascops asio*)	O, F, VI, H
Antarctic Prion (*Pachyptila desolata*)	O
Fairy Prion (*P. turtur*)	O
Broad-billed Prion (*P. vittata*)	O
Common Diving-Petrel (*Pelecanoides urinatrix*)	O
American White Pelican (*Pelecanus erythrorhynchos*)	O, S, F
Great White Pelican (*P. onocrotalus*)	O
Visayan Tarictic Hornbill (*Penelopides panini*)	O
White-tailed Tropicbird (*Phaethon lepturus*)	O
European Shag (*Phalacrocorax aristotelis*)	O
Double-crested Cormorant (*P. auritus*)	O, F, VI, H
Great Cormorant (*P. carbo*)	O
Laysan Albatross (*Phoebastria immutabilis*)	O, F, µCT
Great Auk (*Pinguinus impennis*)	O
Great Crested Grebe (*Podiceps cristatus*)	O
Pale-winged Trumpeter (*Psophia leucoptera*)	O
Bonin Petrel (*Pterodroma hypoleuca*)	O
Atlantic Petrel (*P. incerta*)	O, S
Black-necked Aracari (*Pteroglossus aracari*)	O
Adélie Penguin (*Pygoscelis adeliae*)	O, S
African Skimmer (*Rhynchops flavirostris*)	O
Black Skimmer (*R. niger*)	O
Red-winged Tinamou (*Rhynchotus rufescens*)	O
Comb Duck (*Sarkidiornis melanotos*)	O, S
Common Eider (*Somateria mollissima*)	O, S
King Eider (*S. spectabilis*)	O
Humboldt Penguin (*Spheniscus humboldti*)	O
Caspian Tern (*Sterna caspia*)	O
Ostrich (*Struthio camelus*)	O
Masked Booby (*Sula dactylatra*)	O
Great Tinamou (*Tinamus major*)	O
Red-billed Hornbill (*Tockus erythrorhynchus*)	O
Eastern Yellow-billed Hornbill (*T. flavirostris*)	F, µCT
Eurasian Blackbird (*Turdus merula*)	O
Thick-billed Murre (*Uria lomvia*)	O
Sabine's Gull (*Xema sabini*)	O